JACS
JOURNAL OF THE AMERICAN CHEMICAL SOCIETY
Communication
pubs.acs.org/JACS

Mn-Doped Quantum Dot Sensitized Solar Cells: A Strategy to Boost Efficiency over 5%

Pralay K. Santra and Prashant V. Kamat*

Radiation Laboratory, Departments of Chemistry & Biochemistry, and Chemical & Biomolecular Engineering, University of Notre Dame, Notre Dame, Indiana 46556, United States

ABSTRACT: To make Quantum Dot Sensitized Solar Cells (QDSC) competitive, it is necessary to achieve power conversion efficiencies comparable to other emerging solar cell technologies. By employing Mn^{2+} doping of CdS, we have now succeeded in significantly improving QDSC performance. QDSC constructed with Mn-doped-CdS/CdSe deposited on mesoscopic TiO_2 film as photoanode, Cu_2S/Graphene Oxide composite electrode, and sulfide/polysulfide electrolyte deliver power conversion efficiency of 5.4%.

Quantum dot sensitized solar cells (QDSC) are gaining attention as they show promise toward the development of next generation solar cells.[1−5] The versatile properties of semiconductor quantum dots such as tunability of the bandgap,[6,7] high absorption coefficient,[8] generation of multiple electron carriers under high energy excitation,[9] and delivery of hot electrons[10,11] make them attractive candidates for QDSC. The design of QDSCs which is similar to that of dye sensitized solar cell (DSSC) includes deposition of narrow bandgap semiconductor nanocrystals such as CdSe on mesoscopic TiO_2 films.[12] Upon bandgap excitation of the nanostructured semiconductor, the electrons are injected into TiO_2. Although the photocurrent achieved from QDSCs is comparable to that of DSSCs, the observed power conversion efficiency remains quite low because of the low open circuit potential as well as low fill factor. The I_3^-/I^- based electrolyte which is commonly used in DSSCs is unsuitable for QDSCs as it induces corrosion at the working electrode.[12,13]

Recent efforts to improve the power conversion efficiency include use of bilayer electrodes and sensitizing metal chalcogenides with infrared dyes.[14−16] Another approach of modifying intrinsic property of semiconductor nanocrystals is to introduce dopants.[17,18] By doping optically active transition metal ions, for example, Mn^{2+}, it is possible to modify the electronic and photophysical properties of QDs.[19−23] The dopant creates electronic states in the midgap region of the QD thus altering the charge separation and recombination dynamics. In addition, it is also possible to tune the optical and electronic properties of semiconductor nanocrystals by controlling the type and concentration of dopants. Synthesis of Mn doped II−VI semiconductor-QDs and their photophysical properties have been the subject of recent reports.[24−26] Mn doped CdS, ZnS, and ZnSe show emission at ∼585 nm due to the Mn d−d transition ($^4T_1$−$^6A_1$). However, this transition is both spin and orbitally forbidden resulting in a very long lifetime in the range of several hundreds of microseconds.[22,27,28] Thus, it should be advantageous to utilize long-lived charge carriers to boost the efficiency of solar cells using Mn-doped-quantum dots (Figure 1). Surprisingly, little effort has been made to utilize such doped semiconductor QDs in solar cells.

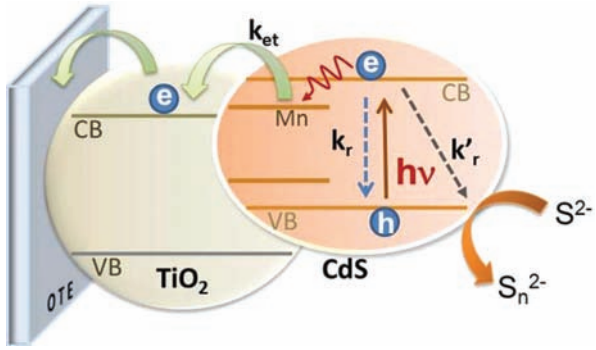

Figure 1. Schematic diagram illustrating the electron transfer (k_{et}) from doped CdS into TiO_2 nanoparticles. k_r and k'_r represent electron recombination with holes and redox couple, respectively.

We have now succeeded in doping CdS semiconductor films with Mn^{2+} for designing high efficiency solar cells. The study marks an important milestone in overcoming the barrier of achieving power conversion efficiency (PEC) greater than 5%.

The photoactive semiconductor electrodes were prepared by successive ionic layer adsorption and reaction (SILAR) method.[29−31] In brief, 0.1 M cadmium nitrate in methanol was used as cation source and 0.1 M sodium sulfide in 1:1 methanol and water as anion source. To incorporate doping of Mn^{2+}, manganese acetate (0.075 M) was mixed with cadmium nitrate. This allowed coadsorption of Mn^{2+} and Cd^{2+} ions, which in turn facilitated incorporation of Mn^{2+} in the CdS film. Each cycle of SILAR consists of successive immersion of the FTO glass electrode, precoated with transparent active TiO_2 layer and a scattering layer,[14,32] in metal ion and sulfide (or selenide) anion solutions for 1 min. The cadmium and selenide ion precursor solution for CdSe was prepared by mixing 0.03 M cadmium nitrate and 0.03 M selenium oxide, respectively, with 0.06 M sodium borohydride, in degassed ethanol inside a glove box under N_2 atmosphere. All the working electrodes were finally coated with 2 cycles of ZnS. The counter electrode was prepared by doctor blading Cu_2S and reduced graphene oxide (RGO) composite on FTO glass.[32] A solution of 1 M sodium

Received: November 30, 2011
Published: January 23, 2012

   dx.doi.org/10.1021/ja211224s | J. Am. Chem.Soc. 2012, 134, 2508−2511

sulfide and 1 M sulfur dissolved in water was used as the liquid electrolyte. The cells were assembled in sandwich fashion using a parafilm spacer. Solar cell performance was evaluated under simulated AM1.5 irradiation conditions.

We prepared four different types of semiconductor photoanodes: (a) 10 SILAR cycles of undoped CdS, (b) 10 SILAR cycles of Mn-doped-CdS, (c) 5 cycles of undoped CdS followed by 8 cycles of CdSe (CdS/CdSe), and (d) 5 cycles of Mn-doped CdS followed by 8 cycles of CdSe (Mn-doped-CdS/CdSe). The normalized absorption spectra of these electrodes and corresponding photographs of the photoanodes are shown in the main panel of Figure 2.

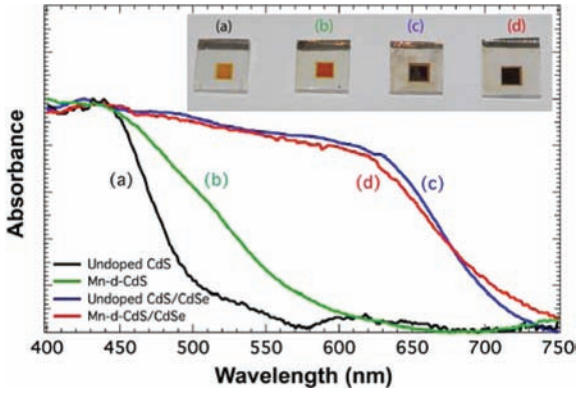

Figure 2. Diffuse reflectance absorbance spectra of semiconductor films deposited on mesoscopic TiO_2 films: (a) undoped CdS, (b) Mn doped CdS, (c) undoped CdS/CdSe, and (d) Mn doped CdS/CdSe. The spectra were normalized for absorbance at 450 nm. Inset shows a photograph of the corresponding four semiconductor films deposited on active TiO_2 layers.

The absorption spectra of CdS deposited film (spectrum a, Figure 2) shows absorption onset around 520 nm, which corresponds to a bandgap of 2.4 eV. The Mn-doped-CdS shows a red-shift in the absorption with onset around 570 nm. The absorption of both undoped and Mn-doped-CdS/CdSe shifts further into the red region with absorption onset below 690 nm. The black-brown color of the films further ascertain the ability to capture all incident photons.

The incident-photon-to-carrier conversion-efficiency (IPCE) recorded at different incident light wavelengths for QDSC that employ four different photoactive semiconductor electrodes is shown in Figure 3. The overall photocurrent response matches the absorption features with photocurrent onsets around 600 nm for CdS and 700 nm for CdS/CdSe electrodes. Both doped and undoped CdS exhibit broad response with maximum IPCE around 60%. The longer wavelength response of Mn-doped CdS parallels the behavior seen in the absorption spectra. Significant enhancement in the IPCE is seen for CdS/CdSe films with maximum IPCE in the range of 68−80%. The broad absorption in the visible and highest photoconversion efficiency highlights the importance of Mn-doping of the metal chalcogenide films. The 7.5% Mn^{2+} solution employed for incorporating Mn dopants in CdS films is optimized for the best performance (The actual Mn concentration in the CdS film as measured from the Inductively Coupled Plasma Atomic Emission Spectroscopy, ICP-AES, analysis was found to be 0.8%). Higher concentration of Mn-doping did not improve the performance.

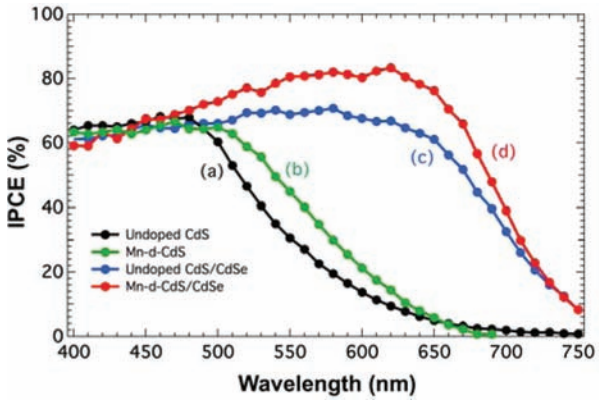

Figure 3. IPCE spectra for (a) CdS, (b) Mn-doped-CdS, (c) CdS/CdSe, and (d) Mn-doped-CdS/CdSe (Cu_2S/RGO counter electrode and aqueous 1 M S^{2-}/1 M S as electrolyte).

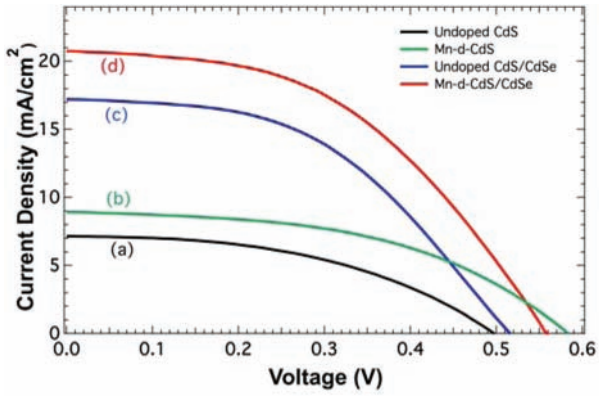

Figure 4. $J-V$ characteristics of different working electrodes measured under AM 1.5 global filter of 100 mW/cm^2 sunlight: (a) undoped CdS, (b) Mn-doped-CdS, (c) undoped CdS/CdSe, and (d) Mn-doped-CdS/CdSe. The working electrodes areas were 0.20, 0.20, 0.22, and 0.22 cm^2, respectively (Cu_2S/RGO counter electrode and aqueous 1 M S^{2-}/1 M S as electrolyte).

The $J-V$ characteristics of these four QDSCs are presented in Figure 4. The short circuit current, open circuit voltage, fill factor, and power conversion efficiency of doped and undoped systems are summarized in Table 1. The open circuit voltage

Table 1. Different Photovoltaics Parameters for Different Working Electrodes

sample	J_{SC} (mA/cm^2)	V_{OC} (mV)	*ff*	η (%)
CdS	7.2	496	0.46	1.63
Mn-d-CdS	8.9	583	0.49	2.53
CdS/CdSe	17.2	516	0.47	4.19
Mn-d-CdS/CdSe	20.7	558	0.47	5.42

for CdS and CdS/CdSe is around 0.5 V. However, an increase in the photovoltage is seen in the Mn-doped CdS (V_{OC} = 583 mV) and CdS/CdSe (558 mV) films. Similarly, Mn-doped films also exhibited significant increase (20%) in the photocurrent as compared to the corresponding semiconductor films without dopants. The fill factor remained constant for all four QDSC, implying similar electrochemical limitations during conversion of light into electricity. The increase seen in the short circuit current and the open circuit voltage with Mn-doped system is reflected in the overall power conversion

dx.doi.org/10.1021/ja211224s | J. Am. Chem.Soc. 2012, 134, 2508−2511

efficiency. The efficiency of 5.42% obtained with Mn-doped CdS/CdSe film is one of the highest performing QDSC reported to date. Other efforts to design bulk heterojunction quantum dot solar cells with Sb_2S_3, PbS, and PbSe have yielded efficiencies in the range of 5−5.5%.[33−36] The enhancement in the photoelectrochemical performance seen with quantum dot sensitization of TiO_2 is another milestone for achieving efficiencies greater than 5%.

The photostability for Mn-doped-CdS/CdSe was measured for 2 h under the continuous illumination (Figure 5). During the first 2 h of illumination, we observe delivery of steady photocurrent from the QDSC. The drop in photocurrent is less than 2% during this initial period of illumination. A water filter was used to filter out infrared and avoid any evaporation of the electrolyte. With a proper sealant, it should be possible to avoid electrolyte evaporation during long-term irradiation.

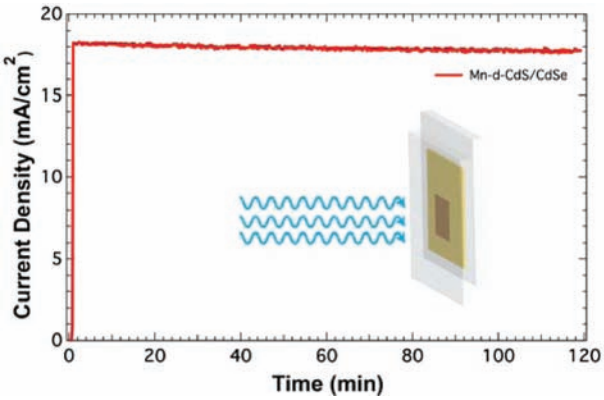

Figure 5. Photocurrent stability of Mn-doped-CdS/CdSe under continuous illumination of 100 mW/cm^2. Inset shows the schematic design of the sandwich-solar cell (Cu_2S/RGO counter electrode and aqueous 1 M S^{2-}/1 M S as electrolyte).

The factors limiting the power conversion efficiency in QDSC include recombination of charge carriers with redox couple at the semiconductor interface, slower hole transfer, and counter electrode performance.[1] Our earlier effort to design Cu_2S/graphene oxide counter electrode has already resulted in significant enhancement in the fill factor of the QD.[32] The charge injection from excited semiconductor into TiO_2 is usually an ultrafast process occurring within few picoseconds.[37] However, slower hole transfer to sulfide redox couple makes the charge recombination a major limiting factor in achieving higher efficiency of QDSC.[38] The midgap states created by Mn-doping cause electrons to get trapped and screen it from charge recombination with holes and/or oxidized polysulfide electrolyte (Figure 1). Indeed, improved photovoltage of the QDSC with doped semiconductor films indicates that Mn-doping assists in electron accumulation within the film, thus shifting the Fermi level to more negative potentials. Efforts are underway to study the charge transfer dynamics and recombination processes in doped semiconductor-TiO_2 systems.

In summary, the doping of CdS/CdSe films with Mn has enabled us to achieve nearly 20% enhancement in the power conversion efficiency as compared to undoped films. The success of crossing the power conversion efficiency barrier of 5% for QDSC shows its potential toward competing with other emerging solar cells such as dye sensitized solar cells and organic photovoltaic cells.

AUTHOR INFORMATION

Corresponding Author

pkamat@nd.edu

Notes

The authors declare no competing financial interest.

ACKNOWLEDGMENTS

The research described herein was supported by the Office of Basic Energy Sciences of U.S. Department of Energy (DE-FC02-04ER15533). We also would like to acknowledge Center for Environmental Science & Technology, University of Notre Dame, for the access of analytical facilities. This is contribution NDRL 4906 from the Notre Dame Radiation Laboratory. We acknowledge Ben Meekins, Hyunbong Choi, and James Radich for fruitful scientific discussions.

REFERENCES

(1) Kamat, P. V.; Tvrdy, K.; Baker, D. R.; Radich, J. G. *Chem. Rev.* **2010**, *110*, 6664−6688.
(2) Kamat, P. V. *J. Phys. Chem. C* **2008**, *112*, 18737−18753.
(3) Mora-Sero, I.; Bisquert, J. *J. Phys. Chem. Lett.* **2010**, *1*, 3046−3052.
(4) Hodes, G. *J. Phys. Chem. C* **2008**, *112*, 17778−17787.
(5) Kramer, I. J.; Sargent, E. H. *ACS Nano* **2011**, *5*, 8506−8514.
(6) Murray, C. B.; Norris, D. J.; Bawendi, M. G. *J. Am. Chem. Soc.* **1993**, *115*, 8706−8715.
(7) Sarma, D. D.; Nag, A.; Santra, P. K.; Kumar, A.; Sapra, S.; Mahadevan, P. *J. Phys. Chem. Lett.* **2010**, *1*, 2149−2153.
(8) Yu, W. W.; Qu, L. H.; Guo, W. Z.; Peng, X. G. *Chem. Mater.* **2004**, *16*, 560−560.
(9) Beard, M. C. *J. Phys. Chem. Lett.* **2011**, *2*, 1282−1288.
(10) Pandey, A.; Guyot-Sionnest, P. *J. Phys. Chem. Lett.* **2010**, *1*, 45−47.
(11) Tisdale, W. A.; Williams, K. J.; Timp, B. A.; Norris, D. J.; Aydil, E. S.; Zhu, X. Y. *Science* **2010**, *328*, 1543−1547.
(12) Rowley, J. G.; Farnum, B. H.; Ardo, S.; Meyer, G. J. *J. Phys. Chem. Lett.* **2010**, *1*, 3132−3140.
(13) Call, F.; Stolwijk, N. A. *J. Phys. Chem. Lett.* **2010**, *1*, 2088−2093.
(14) Choi, H.; Nicolaescu, R.; Paek, S.; Ko, J.; Kamat, P. V. *ACS Nano* **2011**, *5*, 9238−9245.
(15) Buhbut, S.; Itzhakov, S.; Oron, D.; Zaban, A. *J. Phys. Chem. Lett.* **2011**, *2*, 1917−1924.
(16) Buhbut, S.; Itzhakov, S.; Tauber, E.; Shalom, M.; Hod, I.; Geiger, T.; Garini, Y.; Oron, D.; Zaban, A. *ACS Nano* **2010**, *4*, 1293−1298.
(17) Pradhan, N.; Sarma, D. D. *J. Phys. Chem. Lett.* **2011**, *2*, 2818−2826.
(18) Chikan, V. *J. Phys. Chem. Lett.* **2011**, *2*, 2783−2789.
(19) Bhargava, R. N.; Gallagher, D.; Hong, X.; Nurmikko, A. *Phys. Rev. Lett.* **1994**, *72*, 416−419.
(20) Jana, S.; Srivastava, B. B.; Pradhan, N. *J. Phys. Chem. Lett.* **2011**, *2*, 1747−1752.
(21) Beaulac, R.; Archer, P. I.; Ochsenbein, S. T.; Gamelin, D. R. *Adv. Funct. Mater.* **2008**, *18*, 3873−3891.
(22) Beaulac, R.; Archer, P. I.; Gamelin, D. R. *J. Solid State Chem.* **2008**, *181*, 1582−1589.
(23) Zeng, R.; Rutherford, M.; Xie, R.; Zou, B.; Peng, X. *Chem. Mater.* **2010**, *22*, 2107−2113.
(24) Norris, D. J.; Efros, A. L.; Erwin, S. C. *Science* **2008**, *319*, 1776−1779.
(25) Karan, N. S.; Sarma, D. D.; Kadam, R. M.; Pradhan, N. *J. Phys. Chem. Lett.* **2010**, 2863−2866.
(26) Nag, A.; Cherian, R.; Mahadevan, P.; Gopal, A. V.; Hazarika, A.; Mohan, A.; Vengurlekar, A. S.; Sarma, D. D. *J. Phys. Chem. C* **2010**, *114*, 18323−18329.

(27) Beaulac, R.; Archer, P. I.; Liu, X. Y.; Lee, S.; Salley, G. M.; Dobrowolska, M.; Furdyna, J. K.; Gamelin, D. R. *Nano Lett.* **2008**, *8*, 1197−1201.
(28) Vlaskin, V. A.; Janssen, N.; van Rijssel, J.; Beaulac, R.; Gamelin, D. R. *Nano Lett.* **2010**, *10*, 3670−3674.
(29) Sankapal, B. R.; Mane, R. S.; Lokhande, C. D. *MRS Bull.* **2000**, *35*, 177−184.
(30) Lee, H.; Wang, M. K.; Chen, P.; Gamelin, D. R.; Zakeeruddin, S. M.; Grätzel, M.; Nazeeruddin, M. K. *Nano Lett.* **2009**, *9*, 4221−4227.
(31) Prabakar, K.; Seo, H.; Son, M.; Kim, H. *Mater. Chem. Phys.* **2009**, *117*, 26−28.
(32) Radich, J. G.; Dwyer, R.; Kamat, P. V. *J. Phys. Chem. Lett.* **2011**, *2*, 2453−2460.
(33) Pattantyus-Abraham, A. G.; Kramer, I. J.; Barkhouse, A. R.; Wang, X.; Konstantatos, G.; Debnath, R.; Levina, L.; Raabe, I.; Nazeeruddin, M. K.; Grätzel, M.; Sargent, E. H. *ACS Nano* **2010**, *4*, 3374−3380.
(34) Chang, J. A.; Rhee, J. H.; Im, S. H.; Lee, Y. H.; Kim, H.-j.; Seok, S. I.; Nazeeruddin, M. K.; Gratzel, M. *Nano Lett.* **2010**, *10*, 2609−2612.
(35) Moon, S.-J.; Itzhaik, Y.; Yum, J.-H.; Zakeeruddin, S. M.; Hodes, G.; Gratzel, M. *J. Phys. Chem. Lett.* **2010**, *1*, 1524−1527.
(36) Gao, J.; Perkins, C. L.; Luther, J. M.; Hanna, M. C.; Chen, H.-Y.; Semonin, O. E.; Nozik, A. J.; Ellingson, R. J.; Beard, M. C. *Nano Lett.* **2011**, *11*, 3263−3266.
(37) Tvrdy, K.; Frantszov, P.; Kamat, P. V. *Proc. Natl. Acad. Sci. U.S.A.* **2011**, *108*, 29−34.
(38) Chakrapani, V.; Baker, D.; Kamat, P. V. *J. Am. Chem. Soc.* **2011**, *133*, 9607−9615.